Extremum Seeking for Resonant Frequency Seeking

1 Mass-spring-damper system and resonant frequency

Consider the forced mass-spring-damper system shown in Figure 1 with mass m, spring constant k, damper constant c, external input force $f \in \mathbb{R}$, and displacement $y \in \mathbb{R}$. Suppose that the spring is relaxed when $y = 0$. Then, for all $t \geq 0$, the equations of motion of the forced mass-spring-damper system are given by

$$\ddot{y} = -\frac{k}{m}y - \frac{c}{m}\dot{y} + \frac{1}{m}f \tag{1}$$

$$= -\omega_{\mathrm{n}}^2 y - 2\zeta\omega_{\mathrm{n}}\dot{y} + b_0 f, \tag{2}$$

where $\omega_{\mathrm{n}} \triangleq \sqrt{\frac{k}{m}}$ and $\zeta \triangleq \frac{c}{2\sqrt{mk}}$ are the natural frequency and the damping ratio of the mass-spring-damper system, respectively, and $b_0 \triangleq 1/m$ is an input gain.

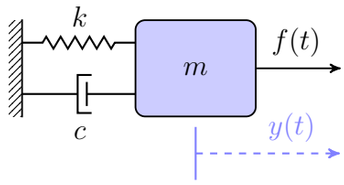

Figure 1: Forced mass-spring-damper system with mass m, spring constant k, damper constant c, external input force $f \in \mathbb{R}$, and displacement $y \in \mathbb{R}$. The effect of gravity is not considered in this system.

It follows from (2) that the transfer function G from f to y is given by

$$G(s) = \frac{b_0}{s^2 + 2\zeta\omega_{\mathrm{n}}s + \omega_{\mathrm{n}}^2}, \tag{3}$$

where $s \in \mathbb{C}$ is the Laplace operator. The frequency response of the mass-spring-damper system can be obtained by setting $s = \jmath\omega$ in (3), where $\omega \geq 0$ is the input frequency. Thus, the gain of the frequency response is given by

$$|G(\jmath\omega)| = \frac{|b_0|}{\sqrt{\omega^4 - 2\omega_{\mathrm{n}}^2(1 - 2\zeta^2)\omega^2 + \omega_{\mathrm{n}}^4}}. \tag{4}$$

Next, define the resonant frequency ω_{r} as

$$\omega_{\mathrm{r}} \triangleq \operatorname*{argmax}_{\omega \geq 0} |G(\jmath\omega)| = \begin{cases} \omega_{\mathrm{n}}\sqrt{1 - 2\zeta^2} & \zeta \leq \frac{1}{\sqrt{2}} \\ 0 & \text{otherwise} \end{cases}. \tag{5}$$

Hence, in the case where $\zeta \leq 1/\sqrt{2}$ and $f = A\sin(\omega t)$ for all $t \geq 0$, where $A > 0$ and $\omega > 0$ are the amplitude and the frequency of the sinusoidal function, respectively, the maximum amplitude of y for a fixed value of A is obtained in the case where $\omega = \omega_{\mathrm{r}}$. In this case, (1) and (2) can be written as

$$\ddot{y} = -\frac{k}{m}y - \frac{c}{m}\dot{y} + \frac{A}{m}\sin(\omega t)$$

$$= -\omega_{\mathrm{n}}^2 y - 2\zeta\omega_{\mathrm{n}}\dot{y} + b_0 A\sin(\omega t). \tag{6}$$

Figure 2 shows the magnitude of the frequency response in the case where $m = 1$ kg, $k = 10^3$ N/m, and $c = 2$ N/(m $\cdot$ s), in which a red, vertical, dashed line is placed at the frequency at which $\omega = \omega_{\mathrm{n}}$.

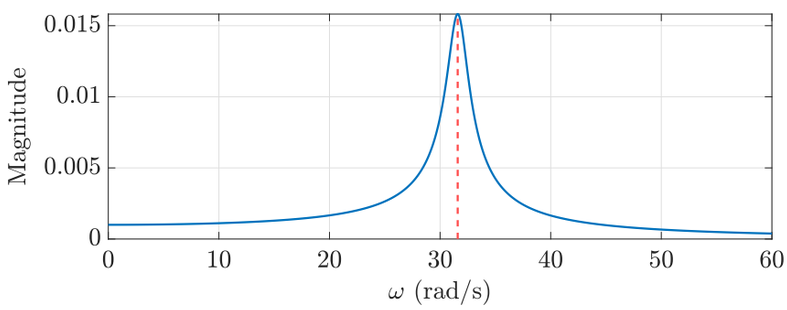

Figure 2: Magnitude of frequency response of the mass-spring-damper system in the case where $m = 1$ kg, $k = 10^3$ N/m, and $c = 2$ N/(m $\cdot$ s). In this case, $\omega_{\mathrm{n}} = 31.62$ rad/s, $\zeta = 0.03$, and $\omega_{\mathrm{r}} = 32.62$ rad/s. A red, vertical, dashed line is placed at the frequency at which $\omega = \omega_{\mathrm{r}}$.

Objective: In the case where $\zeta \leq 1/\sqrt{2}$, $f = A\sin\omega t$ for all $t \geq 0$, and A is fixed, obtain a value of ω that maximizes the amplitude of y with no prior knowledge of m, k, and c, and thus ω_{r}. Hence, extremum seeking control (ESC) is implemented to modulate the input frequency for output amplitude maximization. In this work, both continuous-time (CT) and discrete-time (DT) formulations of extremum seeking control are implemented.

2 Continuous-time extremum seeking control for resonant frequency seeking

Continuous-time extremum seeking control (CT/ESC) is implemented to obtain the resonant frequency of the mass-spring-damper system without prior knowledge of the system properties m, k, c. For this purpose, a control architecture is designed for CT/ESC to modulate the frequency of f to maximize the amplitude of y, composed of a nonlinear oscillator for frequency modulation and a continuous-time, moving root mean square (CT/M-RMS) filter. In this section, the components of this architecture and the manner in which these are interconnected are introduced. Subsection 2.1 introduces the CT nonlinear oscillator for frequency modulation, Subsection 2.2 introduces the CT/M-RMS, filter, Subsection 2.3 introduces CT/ESC, and Subsection 2.4 presents the CT, resonant frequency seeking control architecture, which integrates the previously mentioned components and is shown in Figure 3.

2.1 Continuous-time, nonlinear oscillator

A continuous-time, nonlinear oscillator is considered to obtain a sinusoidal signal with time-varying frequency. The oscillator is based on the Roup oscillator [1, 2] and its dynamics are given by

$$\dot{x}_{\text{osc}} = \left(\begin{bmatrix} 0 & \omega_{\text{cmd}} \\ -\omega_{\text{cmd}} & 0 \end{bmatrix} - \lambda \left(x_{\text{osc}}^{\text{T}} x_{\text{osc}} - A_{\text{cmd}}^2 \right) I_2 \right) x_{\text{osc}}, \tag{7}$$

$$y_{\text{osc}} = \begin{bmatrix} 1 & 0 \end{bmatrix} x_{\text{osc}}, \tag{8}$$

where

- $x_{\text{osc}} \in \mathbb{R}^2$ is the oscillator internal state,
- $y_{\text{osc}} \in \mathbb{R}$ is the oscillator output,
- λ_{osc} is an amplitude convergence rate factor,
- $A_{\text{cmd}} > 0$ is the oscillator commanded amplitude,
- $\omega_{\text{cmd}} \in \mathbb{R}$ is the oscillator commanded frequency in rad/s,, and
- $I_2 \in \mathbb{R}^{2\times 2}$ is an identity matrix.

Note that A_{cmd} and ω_{cmd} determine the amplitude and frequency that the oscillator converges to, respectively, and λ_{osc} determines the rate of convergence of the amplitude of y_{osc} to A_{cmd}. Furthermore, note that large changes in A_{cmd} may destabilize the oscillator in the case where numerical integration is used. In this work, A_{cmd} is fixed, $x_{\text{osc}}(0) = \begin{bmatrix} 0 & A_{\text{cmd}} \end{bmatrix}^{\text{T}}$, $\lambda_{\text{osc}} = 1$.

2.2 Continuous-time, moving root mean square filter

An approximation of the amplitude of y is needed for amplitude maximization, which is obtained by calculating the continuous-time, moving root mean square (CT/M-RMS) of y, given by $y_{\text{rms}} \geq 0$. Suppose that $y(t) = 0$ for all $t < 0$. Then, for all $t \geq 0$, y_{rms} is given by

$$\begin{aligned} y_{\text{rms}}(t) &\triangleq \sqrt{\frac{1}{T_{\text{d}}} \int_{t-T_{\text{d}}}^{t} y^2(\tau)\ \text{d}\tau} = \sqrt{\frac{1}{T_{\text{d}}} \left(\int_0^t y^2(\tau)\ \text{d}\tau - \int_0^{t-T_{\text{d}}} y^2(\tau)\ \text{d}\tau \right)} \\ &= \sqrt{\frac{1}{T_{\text{d}}} \left(\int_0^t y^2(\tau)\ \text{d}\tau - \int_{T_{\text{d}}}^t y^2(\tau - T_{\text{d}})\ \text{d}\tau \right)} = \sqrt{\frac{1}{T_{\text{d}}} \left(\int_0^t y^2(\tau)\ \text{d}\tau - \int_0^t y^2(\tau - T_{\text{d}})\ \text{d}\tau \right)} \\ &= \sqrt{\frac{1}{T_{\text{d}}} \int_0^t y^2(\tau) - y^2(\tau - T_{\text{d}})\ \ \text{d}\tau}, \end{aligned} \tag{9}$$

where $T_{\text{d}} > 0$ is the window over which the root mean square is calculated. Then, the dynamics of the CT/M-RMS filter are obtained by rewriting (9) as

$$\dot{x}_{\text{rms}}(t) = y^2(t) - y^2(t - T_{\text{d}}), \tag{10}$$

$$y_{\text{rms}}(t) = \sqrt{\frac{1}{T_{\text{d}}} x_{\text{rms}}(t)}, \tag{11}$$

where $x_{\text{rms}} > 0$ is an internal state. For implementation purposes, the square root in (11) can be omitted. In this work, $x_{\text{rms}}(0) = y_{\text{rms}}(0) = 0$.

2.3 Continuous-time, extremum seeking controller

The continuous-time, extremum seeking control (CT/ESC) in this work extends the implementation shown in Subchapter 5.2 of [3] to include a control input bias term and different amplitudes for the modulation and demodulation dither signals. The dynamics of the considered ESC are given by

$$\dot{x}_{\mathrm{h}}(t) = -\omega_{\mathrm{h}} x_{\mathrm{h}}(t) + \omega_{\mathrm{h}} K_{\mathrm{g}} y_{\mathrm{m}}(t), \tag{12}$$
$$y_{\mathrm{h}}(t) = K_{\mathrm{g}} y_{\mathrm{m}}(t) - x_{\mathrm{h}}(t), \tag{13}$$
$$\dot{y}_{\mathrm{l}}(t) = -\omega_{\mathrm{l}} y_{\mathrm{l}}(t) + \omega_{\mathrm{l}} y_{\mathrm{h}}(t) A_{\mathrm{esc,d}} \sin(\omega_{\mathrm{esc}} t), \tag{14}$$
$$\dot{y}_{\mathrm{esc}}(t) = y_{\mathrm{l}}(t), \tag{15}$$
$$u_{\mathrm{esc}}(t) = K_{\mathrm{esc}} y_{\mathrm{esc}}(t) + A_{\mathrm{esc,m}} \sin(\omega_{\mathrm{esc}} t) + u_0, \tag{16}$$

where

- $y_{\mathrm{m}} \in \mathbb{R}$ is the CT/ESC measurement,
- $K_{\mathrm{g}} > 0$ is a measurement gain,
- $x_{\mathrm{h}}, y_{\mathrm{h}} \in \mathbb{R}$ are the high-pass filter internal state and output, respectively,
- $\omega_{\mathrm{h}} > 0$ is the cutoff frequency of the high-pass filter in rad/s,
- $y_{\mathrm{l}} \in \mathbb{R}$ is the low-pass filter output,
- $\omega_{\mathrm{l}} > 0$ is the cutoff frequency of the low-pass filter in rad/s,
- $\omega_{\mathrm{esc}} > 0$ is the frequency of the CT/ESC dither signals in rad/s,
- $A_{\mathrm{esc,d}}, A_{\mathrm{esc,m}} \geq 0$ are the amplitudes of the CT/ESC demodulation and modulation dither signals, respectively,
- $y_{\mathrm{esc}} \in \mathbb{R}$ is the CT/ESC modulation state,
- $K_{\mathrm{esc}} \in \mathbb{R}$ is the CT/ESC modulation gain,
- $u_0 \in \mathbb{R}$ is the CT/ESC bias term, and
- u_{esc} is the CT/ESC output, and thus the control input.

Note that K_{g} is used to improve the stabilization properties of CT/ESC by amplifying or reducing the amplitude of the measurement signal and to enable the CT/ESC controller, the sign of K_{esc} is chosen to either maximize or minimize y_{m}, and u_0 is chosen as the initial value of the CT/ESC output u_{esc}. Furthermore, note that $A_{\mathrm{esc,m}}$ can be set to zero after u_{esc} reaches a neighborhood near the value that either maximizes or minimizes y_{m} to stop the oscillations in u_{esc}. In this work, $x_{\mathrm{h}}(0) = y_{\mathrm{l}}(0) = y_{\mathrm{esc}}(0) = 0$, which implies that $u_{\mathrm{esc}}(0) = u_0$, and $K_{\mathrm{esc}} > 0$ to maximize y_{m}. The CT/ESC block diagram is shown in Figure 3.

2.4 Continuous-time, resonant frequency seeking control architecture

The control architecture shown in Figure 3 integrates the systems introduced in Subsections 2.1, 2.2, and 2.3 with the mass-spring-damper system introduced in Section 1. For this implementation, the input of the mass-spring-damper system is the output of the nonlinear oscillator, the commanded frequency of the nonlinear oscillator is the output of the CT/ESC block, and the measurement of the CT/ESC block is the output of the CT/M-RMS block, such that, for all $t \geq 0$,

$$f(t) = y_{\mathrm{osc}}(t), \tag{17}$$
$$\omega_{\mathrm{cmd}}(t) = u_{\mathrm{esc}}(t), \tag{18}$$
$$y_{\mathrm{m}}(t) = y_{\mathrm{rms}}(t). \tag{19}$$

Furthermore, the CT/ESC bias term is set as the initial chosen commanded frequency, such that $u_0 = \omega_{\mathrm{cmd}}(0)$.

2.5 Numerical simulation

Consider the case in which $y(0) = \dot{y}(0) = 0$ and the system parameters are given by

$$m = 1 \text{ kg}, \quad k = 1000 \text{ kg/s}^2, \quad c = 2 \text{ kg/s},$$

such that

$$\omega_{\mathrm{n}} = 31.62 \text{ rad/s}, \quad \zeta = 0.03, \quad \omega_{\mathrm{p}} = 31.59 \text{ rad/s}.$$

Next, let the nonlinear oscillator and moving RMS parameters be given by

$$A_{\mathrm{cmd}} = 1, \ T_{\mathrm{d}} = 2 \text{ s}, \tag{20}$$

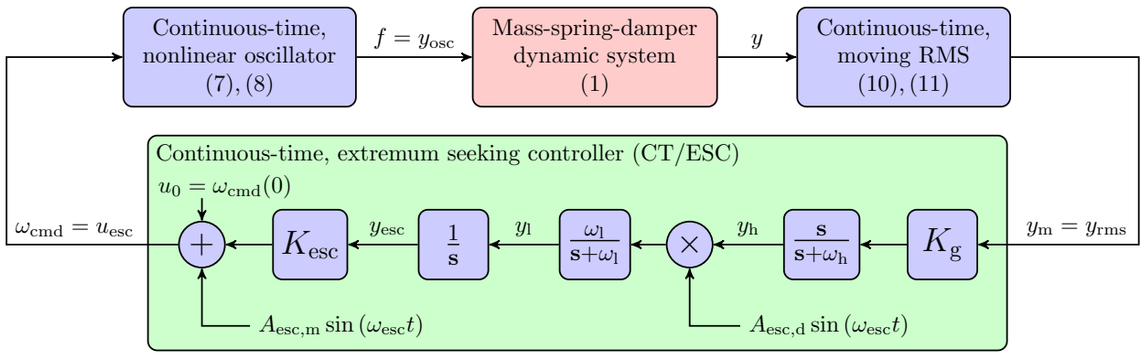

Figure 3: Continuous-time, resonant frequency seeking control architecture applied to mass-spring-damper system. The architecture incorporates the continuous-time nonlinear oscillator, the continuous-time, moving RMS filter, and the CT/ESC dynamics introduced in Subsections 2.1, 2.2, and 2.3.

and let the ESC hyperparameters be given by

$$u_0 = \omega_{\text{cmd}}(0) = 20 \text{ rad/s}, \quad \omega_{\text{l}} = 4 \text{ rad/s}, \quad \omega_{\text{h}} = 2 \text{ rad/s}, \quad \omega_{\text{esc}} = 1 \text{ rad/s}, \quad A_{\text{esc,d}} = 1, \quad K_{\text{esc}} = 2.5, \tag{21}$$

and

$$K_{\text{g}} = \begin{cases} 0, & t < 2T_{\text{d}}, \\ 500, & t \geq 2T_{\text{d}}, \end{cases} \tag{22}$$

$$A_{\text{esc,m}} = \begin{cases} 1, & t \leq 300 \text{ s}, \\ 0, & t > 300 \text{ s}, \end{cases} \tag{23}$$

which implies that ESC will start modulation at $t = 2T_{\text{d}}$ and that $A_{\text{esc,m}}$ becomes zero after $t = 300$ s. The results from running the closed-loop system shown in Figure 3 in Simulink are shown in Figures 4 and 5, which show that the commanded frequency oscillates around the resonant frequency ω_{r} after $t = 250$ s, after which $A_{\text{esc,d}}$ is set to zero to stop the oscillations. The code for running this example is shown in `msd_resonant_frequency_seeking_CT_run.m`.

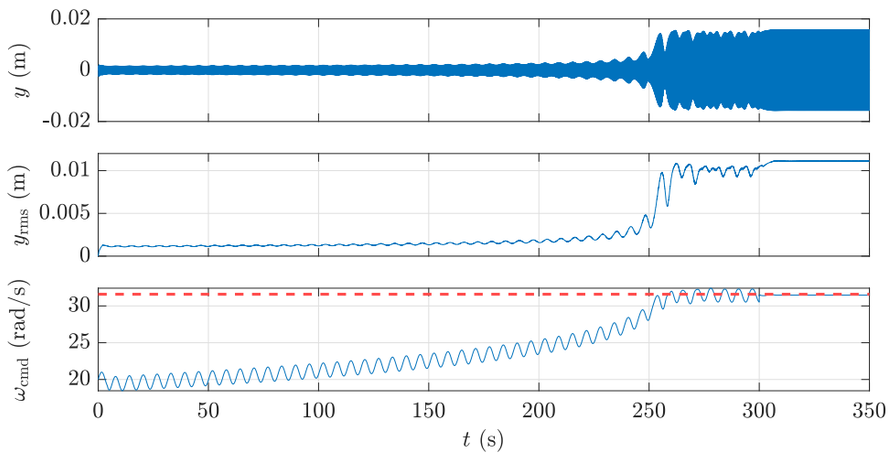

Figure 4: Results of resonant frequency seeking using CT/ESC applied to a mass-spring-damper system. The horizontal, red, dashed line denotes the resonant frequency ω_{r}, which is reached by the output of CT/ESC.

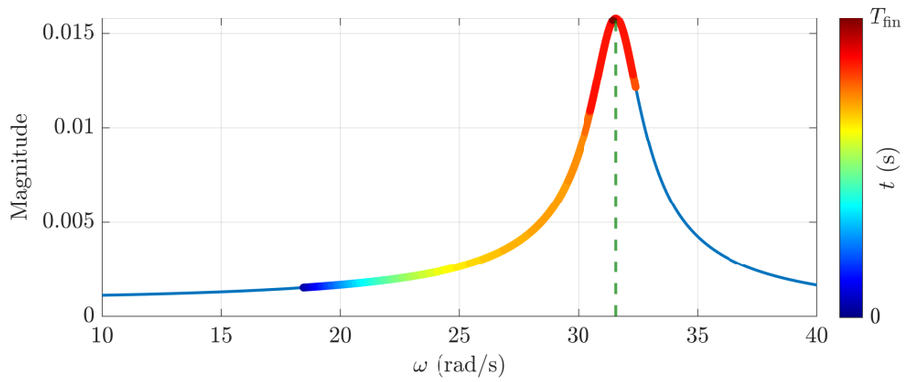

Figure 5: The commanded frequency ω_{cmd} trajectory resulting from the implementation of CT/ESC plotted over the magnitude of the frequency response of the mass-spring-damper system. A green, vertical, dashed line is placed at the frequency at which $\omega = \omega_{\text{r}}$. For this numerical simulation, $T_{\text{fin}} = 350$ s.

3 Discrete-time extremum seeking control for resonant frequency seeking

Discrete-time extremum seeking control (DT/ESC) is implemented to obtain the resonant frequency of the mass-spring-damper system without prior knowledge of the system properties m, k, c. For this purpose, a control architecture is designed for DT/ESC to modulate the frequency of f to maximize the amplitude of y, composed of a nonlinear oscillator for frequency modulation and a discrete-time, moving root mean square (DT/M-RMS) filter. In this section, the components of this architecture and the manner in which these are interconnected are introduced. Subsection 3.1 introduces the DT nonlinear oscillator for frequency modulation, Subsection 3.2 introduces the DT/M-RMS, filter, Subsection 3.3 introduces DT/ESC, and Subsection 3.4 presents the DT, resonant frequency seeking control architecture, which integrates the previously mentioned components and is shown in Figure 6.

Furthermore, while the the discrete-time setup is similar to the continuous-time setup, two different sampling rates are used for the discrete-time setup. Hence, $T_\mathrm{s} > 0$ is used for the nonlinear oscillator and DT/M-RMS, and $T_\mathrm{esc} > 0$ is used for DT/ESC, such that $T_\mathrm{s} < T_\mathrm{esc}$ and $T_\mathrm{esc}/T_\mathrm{s} \in \{1, 2, \ldots\}$. This setup is considered to separate the frequency modulation and oscillation generation processes, since frequency modulation requires a slower update rate to better assess the effect of the generated oscillation on the system output. The sampling indices $\kappa, k \in \{0, 1, \ldots\}$ are associated with T_s and T_esc, respectively.

3.1 Discrete-time, nonlinear oscillator

A discrete-time, nonlinear oscillator is considered to obtain a sinusoidal signal with time-varying frequency, whose dynamics for all $\kappa \geq 0$ are given by

$$x_{\mathrm{osc},\kappa+1} = \left(\begin{bmatrix} \cos(T_\mathrm{s}\omega_{\mathrm{cmd},\kappa}) & \sin(T_\mathrm{s}\omega_{\mathrm{cmd},\kappa}) \\ -\sin(T_\mathrm{s}\omega_{\mathrm{cmd},\kappa}) & \cos(T_\mathrm{s}\omega_{\mathrm{cmd},\kappa}) \end{bmatrix} - \lambda_\mathrm{osc}(x_{\mathrm{osc},\kappa}^\mathrm{T} x_{\mathrm{osc},\kappa} - A_{\mathrm{cmd},\kappa}^2) I_2 \right) x_{\mathrm{osc},\kappa}, \tag{24}$$

$$y_{\mathrm{osc},\kappa} = \begin{bmatrix} 1 & 0 \end{bmatrix} x_{\mathrm{osc},\kappa}, \tag{25}$$

where

- $x_{\mathrm{osc},\kappa} \in \mathbb{R}^2$ is the oscillator internal state,
- $y_{\mathrm{osc},\kappa} \in \mathbb{R}$ is the oscillator output,
- λ_osc is an amplitude convergence rate factor,
- $A_{\mathrm{cmd},\kappa} > 0$ is the oscillator commanded amplitude,
- $\omega_{\mathrm{cmd},\kappa} \in \mathbb{R}$ is the oscillator commanded frequency in rad/s,, and
- $I_2 \in \mathbb{R}^{2\times 2}$ is an identity matrix.

Note that $A_{\mathrm{cmd},\kappa}$ and $\omega_{\mathrm{cmd},\kappa}$ determine the amplitude and frequency that the oscillator converges to, respectively, and λ_osc determines the rate of convergence of the amplitude of $y_{\mathrm{osc},\kappa}$ to $A_{\mathrm{cmd},\kappa}$. Furthermore, note that large changes in $A_{\mathrm{cmd},\kappa}$ may destabilize the oscillator. In this work, $A_{\mathrm{cmd},\kappa}$ is fixed for all $\kappa \geq 0$, such that $A_{\mathrm{cmd},\kappa} \equiv A_\mathrm{cmd}$, $x_{\mathrm{osc},0} = \begin{bmatrix} 0 & A_\mathrm{cmd} \end{bmatrix}^\mathrm{T}$, and $\lambda_\mathrm{osc} = 1$.

3.2 Discrete-time, moving root mean square filter

An approximation of the amplitude of x is obtained by calculating the discrete-time, moving root mean square (DT/M-RMS) of y_κ, which is obtained by sampling y at a rate of T_s. In this work, the DT/M-RMS of y_κ, given by $y_{\mathrm{rms},\kappa} \geq 0$, is given by the square root of the cumulative moving average of y_κ^2, such that, for all $\kappa \geq 0$, the update equations of the DT/M-RMS filter are given by

$$x_{\mathrm{rms},\kappa+1} = x_{\mathrm{rms},\kappa} + \frac{y_\kappa^2 - x_{\mathrm{rms},\kappa}}{\ell_\mathrm{rms} + 1}, \tag{26}$$

$$y_{\mathrm{rms},\kappa} = \sqrt{x_{\mathrm{rms},\kappa}}, \tag{27}$$

where $x_{\mathrm{rms},\kappa} > 0$ is an internal state, and $\ell_\mathrm{rms} > 0$ is the number of samples considered in the cumulative average calculation. As in the CT case, the square root in (27) can be omitted for implementation purposes. In this work, $x_{\mathrm{rms},0} = y_{\mathrm{rms},0} = 0$.

3.3 Discrete-time, extremum seeking controller

The discrete-time, extremum seeking control (DT/ESC) in this work extends the implementation shown in Subchapter 4.2 of [3] to include a control input bias term, a low-pass filter, and different amplitudes for the

modulation and demodulation dither signals. For all $k \geq 0$, the update equations of the considered ESC are given by

$$x_{\mathrm{h},k+1} = -\omega_{\mathrm{h}} T_{\mathrm{esc}} x_{\mathrm{h},k} + (1 + \omega_{\mathrm{h}} T_{\mathrm{esc}}) K_{\mathrm{g}} y_{\mathrm{m},k}, \tag{28}$$

$$y_{\mathrm{h},k} = K_{\mathrm{g}} y_{\mathrm{m},k} - x_{\mathrm{h},k}, \tag{29}$$

$$y_{\mathrm{l},k+1} = -(\omega_{\mathrm{l}} T_{\mathrm{esc}} - 1) y_{\mathrm{l},k} + \omega_{\mathrm{l}} T_{\mathrm{esc}} y_{\mathrm{h},k} A_{\mathrm{esc,d}} \sin(\omega_{\mathrm{esc}} T_{\mathrm{esc}} k), \tag{30}$$

$$y_{\mathrm{esc},k+1} = y_{\mathrm{esc},k} + y_{\mathrm{l},k}, \tag{31}$$

$$u_{\mathrm{esc},k} = K_{\mathrm{esc}} y_{\mathrm{esc},k} + A_{\mathrm{esc,m}} \sin(\omega_{\mathrm{esc}} T_{\mathrm{esc}} k) + u_0, \tag{32}$$

where

- $y_{\mathrm{m},k} \in \mathbb{R}$ is the DT/ESC measurement,
- $K_{\mathrm{g}} > 0$ is a measurement gain,
- $x_{\mathrm{h},k}, y_{\mathrm{h},k} \in \mathbb{R}$ are the high-pass filter internal state and output, respectively,
- $\omega_{\mathrm{h}} > 0$ is the cutoff frequency of the high-pass filter in rad/s,
- $y_{\mathrm{l},k} \in \mathbb{R}$ is the low-pass filter output,
- $\omega_{\mathrm{l}} > 0$ is the cutoff frequency of the low-pass filter in rad/s,
- $\omega_{\mathrm{esc}} > 0$ is the frequency of the DT/ESC dither signals in rad/s,
- $A_{\mathrm{esc,d}}, A_{\mathrm{esc,m}} \geq 0$ are the amplitudes of the CT/ESC demodulation and modulation dither signals, respectively,
- $y_{\mathrm{esc},k} \in \mathbb{R}$ is the DT/ESC modulation state,
- $K_{\mathrm{esc}} \in \mathbb{R}$ is the DT/ESC modulation gain,
- $u_0 \in \mathbb{R}$ is the DT/ESC bias term, and
- $u_{\mathrm{esc},k}$ is the DT/ESC output, and thus the control input.

Similarly to CT/ESC, note that K_{g} is used to improve the stabilization properties of DT/ESC by amplifying or reducing the amplitude of the measurement signal and to enable the DT/ESC controller, the sign of K_{esc} is chosen to either maximize or minimize $y_{\mathrm{m},k}$, and u_0 is chosen as the initial value of the DT/ESC output $u_{\mathrm{esc},k}$. Furthermore, note that $A_{\mathrm{esc,m}}$ can be set to zero after $u_{\mathrm{esc},k}$ reaches a neighborhood near the value that either maximizes or minimizes $y_{\mathrm{m},k}$ to stop the oscillations in $u_{\mathrm{esc},k}$. In this work, $x_{\mathrm{h},0} = y_{\mathrm{l},0} = y_{\mathrm{esc},0} = 0$, which implies that $u_{\mathrm{esc},0} = u_0$, and $K_{\mathrm{esc}} > 0$ to maximize $y_{\mathrm{m},k}$. The DT/ESC block diagram is shown in Figure 6.

3.4 Discrete-time, resonant frequency seeking control architecture

The control architecture shown in Figure 6 integrates the systems introduced in Subsections 3.1, 3.2, and 3.3 with the mass-spring-damper system introduced in Section 1. For this implementation, the signals are sampled, resampled, and converted to continuous-time via the zero-order hold method as needed. The input of the mass-spring-damper system is determined is the output of the nonlinear oscillator, converted to continuous-time by using a zero-order hold method, such that, for all $t \in [\kappa T_{\mathrm{s}}, (\kappa + 1) T_{\mathrm{s}})$,

$$f(t) = y_{\mathrm{osc}}(t) \triangleq y_{\mathrm{osc},\kappa}. \tag{33}$$

The commanded frequency of the nonlinear oscillator is the resampled output of the DT/ESC block, such that, for all $\kappa \in \{0, 1, \ldots\}$,

$$\omega_{\mathrm{cmd},\kappa} = u_{\mathrm{esc}, \left\lfloor \frac{T_{\mathrm{s}}}{T_{\mathrm{esc}}} \kappa \right\rfloor}, \tag{34}$$

where $\lfloor \cdot \rfloor : \mathbb{R} \to \{\ldots, -2, -1, 0, 1, 2, \ldots\}$ is the floor function. The measurement of the DT/ESC block is the resampled output of the DT/M-RMS block, such that, for all $k \geq 0$,

$$y_{\mathrm{m},k} \triangleq y_{\mathrm{rms}, \frac{T_{\mathrm{esc}}}{T_{\mathrm{s}}} k}. \tag{35}$$

Finally, the input of the CT/M-RMS is obtained by sampling y at a rate of T_{s}, such that, for all $\kappa \geq 0$,

$$y_\kappa = y(\kappa T_{\mathrm{s}}). \tag{36}$$

In this work, the DT/ESC bias term is set as the initial chosen commanded frequency, such that $u_0 = \omega_{\mathrm{cmd},0}$.

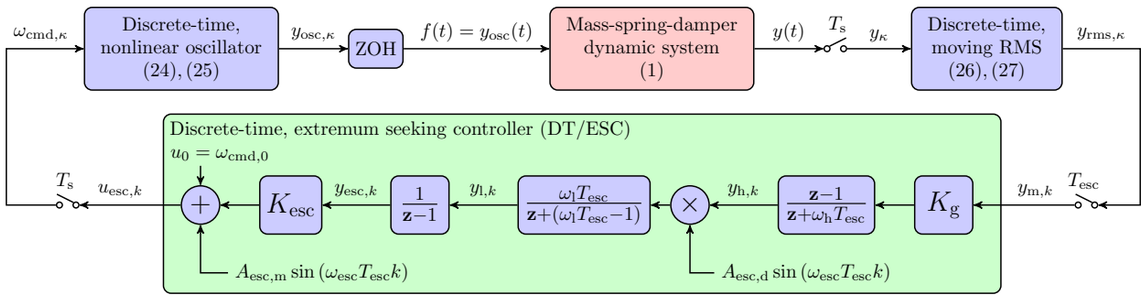

Figure 6: Discrete-time, resonant frequency seeking control architecture applied to mass-spring-damper system. The architecture incorporates the discrete-time nonlinear oscillator, the discrete-time, moving RMS filter, and the DT/ESC update equations introduced in Subsections 3.1, 3.2, and 3.3.

3.5 Numerical simulation

Consider the case in which $y(0) = \dot{y}(0) = 0$ and the system parameters are given by

$$m = 1 \text{ kg}, \quad k = 1000 \text{ kg/s}^2, \quad c = 2 \text{ kg/s},$$

such that

$$\omega_{\mathrm{n}} = 31.62 \text{ rad/s}, \quad \zeta = 0.03, \quad \omega_{\mathrm{p}} = 31.59 \text{ rad/s}.$$

Next, let the sampling rates for the discrete-time setup be given by

$$T_{\mathrm{s}} = 0.001 \text{ s}, \ T_{\mathrm{esc}} = 0.1 \text{ s}, \tag{37}$$

let the nonlinear oscillator and moving RMS parameters be given by

$$A_{\mathrm{cmd}} = 1, \ \ell_{\mathrm{rms}} = 2000, \tag{38}$$

such that $T_{\mathrm{s}}\ell_{\mathrm{s}} = 2$ s, and let the ESC hyperparameters be given by

$$u_0 = \omega_{\mathrm{cmd},0} = 20 \text{ rad/s}, \quad \omega_{\mathrm{l}} = 4 \text{ rad/s}, \quad \omega_{\mathrm{h}} = 0.1 \text{ rad/s}, \quad \omega_{\mathrm{esc}} = 1 \text{ rad/s}, \quad A_{\mathrm{esc,d}} = 1.2, \quad K_{\mathrm{esc}} = 2, \tag{39}$$

and

$$K_{\mathrm{g}} = \begin{cases} 0, & t < 2(\ell_{\mathrm{rms}} + 1)T_{\mathrm{s}}, \\ 500, & t \geq 2(\ell_{\mathrm{rms}} + 1)T_{\mathrm{s}}, \end{cases} \tag{40}$$

$$A_{\mathrm{esc,m}} = \begin{cases} 1.2, & t \leq 300 \text{ s}, \\ 0, & t > 300 \text{ s}, \end{cases} \tag{41}$$

which implies that ESC will start modulation at $t = 2(\ell_{\mathrm{rms}}+1)T_{\mathrm{s}}$ and that $A_{\mathrm{esc,m}}$ becomes zero after $t = 300$ s. The results from running the closed-loop system shown in Figure 6 in Simulink are shown in Figures 7 and 8, which show that the commanded frequency oscillates around the resonant frequency ω_{r} after $t = 250$ s, after which $A_{\mathrm{esc,d}}$ is set to zero to stop the oscillations. The code for running this example is shown in `msd_resonant_frequency_seeking_DT_run.m`.

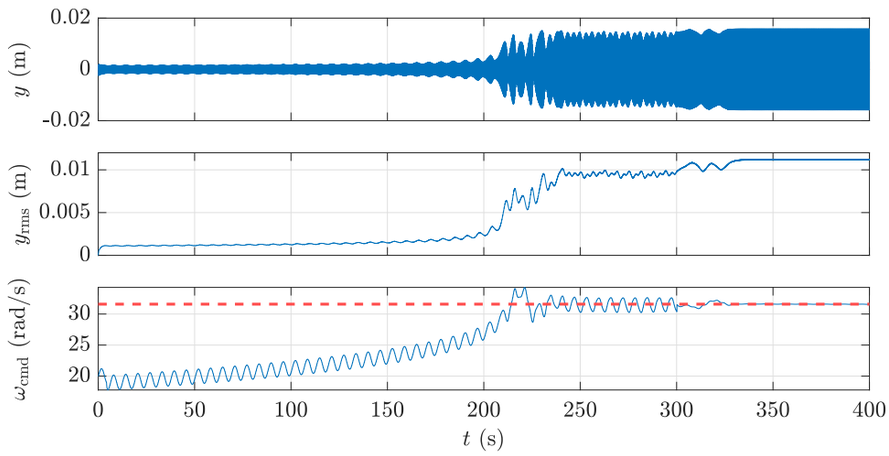

Figure 7: Results of resonant frequency seeking using DT/ESC applied to a mass-spring-damper system. The horizontal, red, dashed line denotes the resonant frequency ω_{r}, which is reached by the output of DT/ESC.

3.6 Vanishing modulation signal dither and numerical simulation

In the previous numerical simulations, the amplitude of the modulation signal was arbitrarily set to zero after reaching a neighborhood around the resonant frequency to allow the ESC output to converge. An alternative approach is to design dynamics for the modulation signal amplitude, such that the amplitude

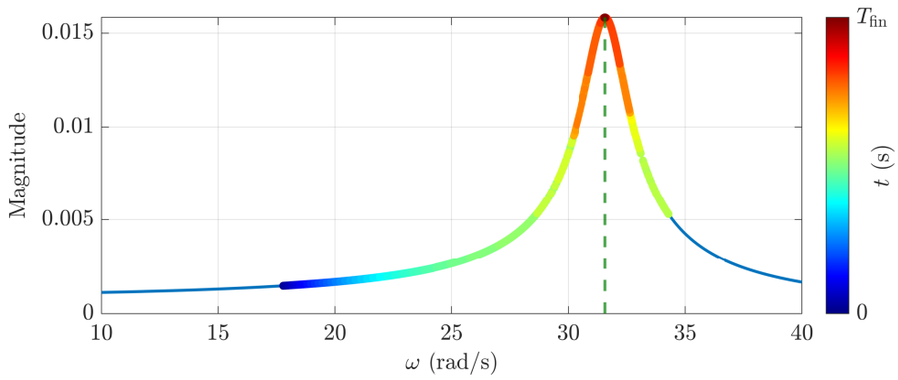

Figure 8: The commanded frequency ω_{cmd} trajectory resulting from the implementation of DT/ESC plotted over the magnitude of the frequency response of the mass-spring-damper system. A green, vertical, dashed line is placed at the frequency at which $\omega = \omega_{\text{r}}$. For this numerical simulation, $T_{\text{fin}} = 400$ s.

converges to zero without user intervention, which yields a vanishing modulation dither. In the case of the DT/ESC implementation, switching dynamics can be assigned to the modulation signal amplitude, such that, for all $k \geq 0$,

$$A_{\text{esc,m},k+1} = \begin{cases} A_{\text{esc,m},0}, & k < k_{\text{en}}, \\ A_{\text{esc,m},k} - \alpha_{\text{m}} y_{\text{l},k} & k \geq k_{\text{en}} \text{ and } \|y_{\text{l},k}\| > \delta_{\text{m}}, \\ A_{\text{esc,m},k} - \lambda_{\text{m}} A_{\text{esc,m},k} & k \geq k_{\text{en}} \text{ and } \|y_{\text{l},k}\| \leq \delta_{\text{m}}. \end{cases} \tag{42}$$

where $A_{\text{esc,m},0} > 0$ is the initial modulation signal amplitude, $k_{\text{en}} \geq 0$ is the DT/ESC step at which DT/ESC is enabled, $\delta_{\text{m}} > 0$ is a switching bound on the norm of $y_{\text{l},k}$, $\alpha_{\text{m}} > 0$ is a gradient descent rate of convergence factor, and $\lambda_{\text{m}} \in (0, 1)$ is an amplitude convergence rate factor. The output of the low-pass filter $y_{\text{l},k}$ is used to determine the dynamics in (42) since its trend determines the average direction in which the output of DT/ESC evolves and becomes close to zero when reaching an extremum, which is the resonant frequency ω_{r} iun this case. Under the dynamics shown in (42), the update equations of $A_{\text{esc,m},k}$ are given by a gradient descent algorithm when $\|y_{\text{l},k}\| > \delta_{\text{m}}$, and become asymptotically stable when $\|y_{\text{l},k}\| \leq \delta_{\text{m}}$.

A numerical simulation in which $A_{\text{esc,m}}$ is given the update equations shown in (42) is presented next. Consider the case in which $y(0) = \dot{y}(0) = 0$ and the system parameters are given by

$$m = 1 \text{ kg}, \quad k = 1000 \text{ kg/s}^2, \quad c = 2 \text{ kg/s},$$

such that

$$\omega_{\text{n}} = 31.62 \text{ rad/s}, \quad \zeta = 0.03, \quad \omega_{\text{p}} = 31.59 \text{ rad/s}.$$

Next, let the sampling rates for the discrete-time setup be given by

$$T_{\text{s}} = 0.001 \text{ s}, \ T_{\text{esc}} = 0.1 \text{ s}, \tag{43}$$

let the nonlinear oscillator and moving RMS parameters be given by

$$A_{\text{cmd}} = 1, \ \ell_{\text{rms}} = 2000, \tag{44}$$

such that $T_{\text{s}}\ell_{\text{s}} = 2$ s, let the ESC hyperparameters be given by

$$u_0 = \omega_{\text{cmd},0} = 20 \text{ rad/s}, \quad \omega_{\text{l}} = 10 \text{ rad/s}, \quad \omega_{\text{h}} = 3 \text{ rad/s}, \quad \omega_{\text{esc}} = 4 \text{ rad/s}, \quad A_{\text{esc,d}} = 1.2, \quad K_{\text{esc}} = 2.5, \tag{45}$$

$$K_{\text{g}} = \begin{cases} 0, & t < 2(\ell_{\text{rms}} + 1)T_{\text{s}}, \\ 500, & t \geq 2(\ell_{\text{rms}} + 1)T_{\text{s}}, \end{cases} \tag{46}$$

which implies that ESC will start modulation at $t = 2(\ell_{\text{rms}} + 1)T_{\text{s}}$, and let the modulation vanishing dither parameters be given by

$$A_{\text{esc,d},0} = 1.2, \ k_{\text{en}} = \lfloor 2(\ell_{\text{rms}} + 1)T_{\text{s}}/T_{\text{esc}} \rfloor, \ \delta_{\text{m}} = 0.002, \ \alpha_{\text{m}} = 0.1, \ \lambda_{\text{m}} = 0.025, \tag{47}$$

where k_{en} corresponds to the ESC modulation start time. The results from running the closed-loop system shown in Figure 6 in Simulink are shown in Figures 9 and 10, which show that the commanded frequency converges to the resonant frequency ω_{r} due to the vanishing dither. The code for running this example is shown in `msd_resonant_frequency_seeking_DT_vanishing_dither_run.m`.

References

[1] A. V. Roup and D. S. Bernstein, "Adaptive stabilization of a class of nonlinear systems with nonparametric uncertainty," *IEEE Trans. Automat. Contr.*, vol. 46, no. 11, pp. 1821–1825, 2001.

[2] A. K. Padthe and D. S. Bernstein, "A delay-Duhem model for jump-resonance hysteresis," in *Proc. Conf. Dec. Contr.*, pp. 1609–1614, IEEE, 2007.

[3] K. B. Ariyur and M. Krstic, *Real-time optimization by extremum-seeking control.* John Wiley & Sons, 2003.

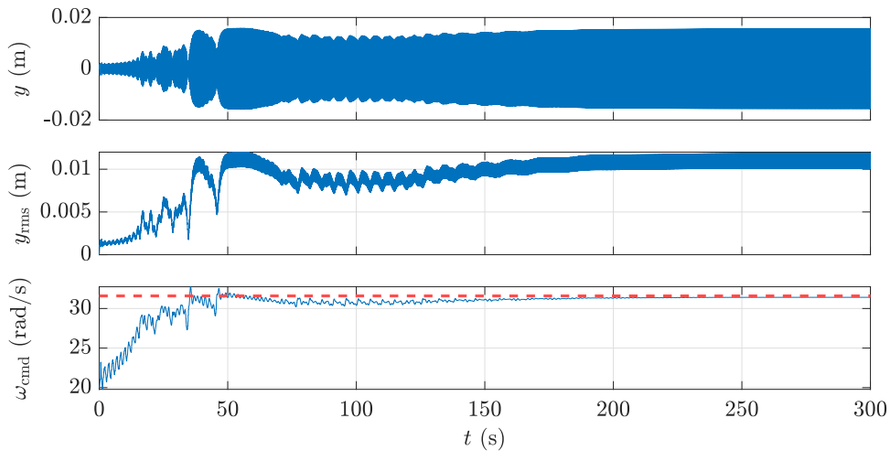

Figure 9: Results of resonant frequency seeking using DT/ESC with a vanishing modulation dither applied to a mass-spring-damper system. The horizontal, red, dashed line denotes the resonant frequency ω_{r}, which is reached by the output of DT/ESC.

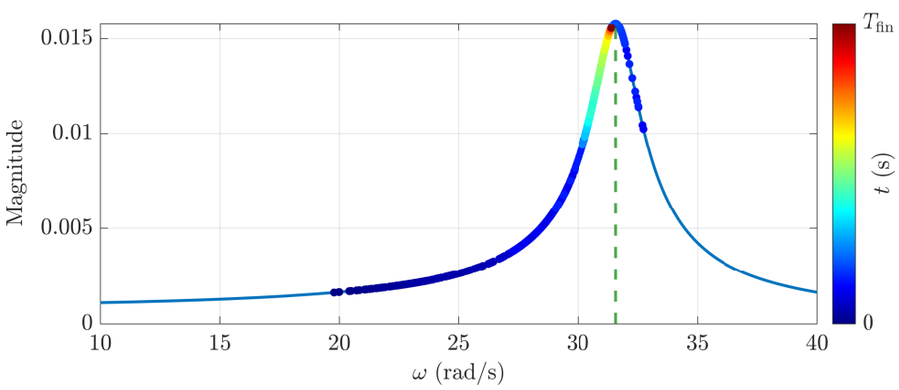

Figure 10: The commanded frequency ω_{cmd} trajectory resulting from the implementation of DT/ESC with a vanishing modulation dither plotted over the magnitude of the frequency response of the mass-spring-damper system. A green, vertical, dashed line is placed at the frequency at which $\omega = \omega_{\mathrm{r}}$. For this numerical simulation, $T_{\mathrm{fin}} = 300$ s.